Pergamon

Int. J. Solids Structures Vol. 33, No. 23, pp. 3463–3476, 1996

0020–7683/96 $15.00 + .00

0020–7683(95)00191–3

ANTI-PLANE ELASTIC WAVE SCATTERING FROM A ROUGH VOLUMETRIC CRACK

PER-ÅKE JANSSON
Division of Mechanics, Chalmers University of Technology, S-412 96 Göteborg, Sweden

(*Received* 30 *November* 1994; *in revised form* 30 *July* 1995)

Abstract—The scattering of elastic waves from cracks is a field of study which has a number of important applications in nondestructive testing (NDT) and characterization of materials. So far most theoretical studies have concerned smooth cracks. There is reason to believe that the influence of roughness will scatter the energy in a more diffuse way, thus complicating the interpretation of test results.

The problem considered here is the scattering of anti-plane waves, i.e. "horizontally" polarized shear waves, from a crack in an otherwise homogeneous, isotropic, elastic solid. The geometry is taken to be two-dimensional, and the scatterer is a curved volumetric crack with a small random roughness, which is characterized by the RMS height and a correlation length which is related to the average distance between the peaks of the irregularities. The term "volumetric" refers to the fact that the crack surfaces are slightly separated. Effects due to overall curvature as well as effects due to surface roughness and separation of the crack surfaces are thus included in the analysis.

The method of solution can be described as an extension of the null field approach where certain matrix elements are expanded in terms of a small parameter describing the deviation from the smooth, nonvolumetric crack. The ensemble averaged amplitude of the scattered field for an incident plane wave has been computed numerically. Some results are given for various values of the frequency, the RMS height, the correlation length and the maximum gap between the crack surfaces. Copyright © 1996 Elsevier Science Ltd

INTRODUCTION

Scattering of waves from various types of flaws (cracks, voids, etc.) in an elastic medium is an area of great interest in a number of practical applications, e.g. nondestructive evaluation. So far, most studies of scattering from cracks have been concerned with smooth surfaces, but it is a well-known fact that the surfaces of most real cracks are more or less rough. The scattering properties are believed to be affected by roughness in the sense that the energy will be scattered in a more diffuse way. According to Ogilvy (1991) scattering from random rough surfaces has been the subject of several books and an "uncountably" large number of research papers. Consequently, it is not possible to give a detailed review of the field here. The reader is referred to the text-book by Ogilvy (1991) for a general overview and further references.

Even though there are numerous papers on scattering from rough surfaces the problem of scattering from rough cracks does not seem to have received so much attention. Some works that may be of interest in this context are the papers by Lewis (1990), Ogilvy and Culverwell (1991) and Boström *et al.* (1994).

In this paper the null field approach is used to solve a two-dimensional problem of scattering from a rough curved crack. The null field approach was originally developed by Waterman (1965) for electromagnetic scattering but has since been extended to acoustic, Waterman (1969), and elastic wave scattering (Pao and Varatharajulu, 1976; Waterman, 1976, 1978). The method was adapted to scattering from smooth cracks in an elastic medium by Boström and Olsson (1987) and further developed by Boström *et al.* (1994) to take the effects of roughness into account.

Normally, when scattering from cracks is considered the volume of the crack is neglected, i.e. the surfaces of the crack are assumed to coincide exactly. For a rough crack this is of course an approximation since we cannot expect the rough surfaces to match completely. In this paper we modify the approach by Boström *et al.* (1994) to take such "volumetric" effects into account. Geometrically similar problems for the scattering of

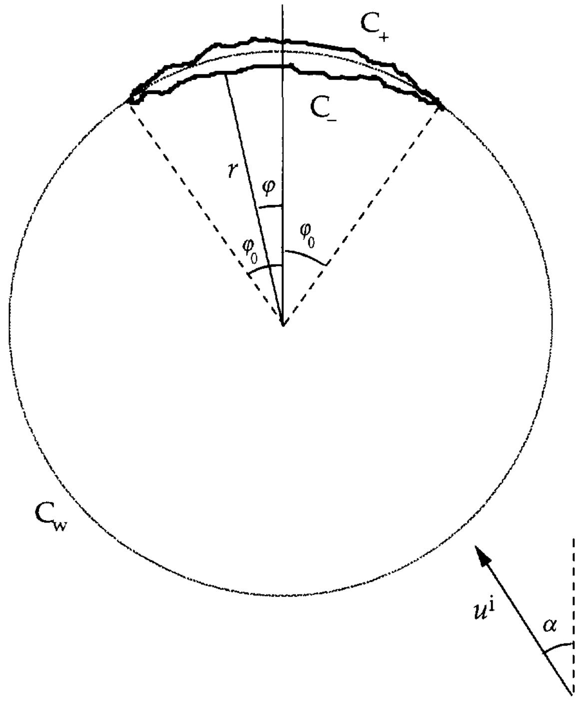

Fig. 1. The geometry of the crack. C_+ and C_- are the boundaries of the two-dimensional crack ; C_w is a fictitious curve that is added to form two closed curves $C_- + C_w$ and $C_{..} + C_w$. α is the angle of incidence of the plane wave.

electromagnetic waves have been treated by Zheng and Ström (1989) using the null field approach.

FORMULATION OF THE PROBLEM AND NULL FIELD SOLUTION

We consider an ensemble of two-dimensional flaws, one of which is shown in Fig. 1 and an incident plane wave in an otherwise linearly elastic, isotropic, homogeneous medium of density ρ and shear modulus μ. The boundary of an individual flaw consists of two distinct portions, C_+ and C_-, which both deviate slightly from a circular arc of radius a and central angle $2\varphi_0$.

It is assumed that C_+ is located outside the arc and C_- inside it, i.e.

$$r = \begin{cases} a+h_+(\varphi) & \text{on } C_+ \\ a-h_-(\varphi) & \text{on } C_- \end{cases} \tag{1}$$

where $0 \leqslant h_\pm(\varphi) \ll a$, for each flaw of the ensemble. Hence, the flaw is not a mathematical crack but has a certain volume. We also assume that the flaw exhibits random surface roughness, the properties of which will be discussed in the following section. The average shape of the surfaces is described by the ensemble averages of the functions $h_\pm(\varphi)$. These are denoted by $\langle h_\pm(\varphi)\rangle \equiv f_\pm(\varphi) \ll a$ and are discussed in the next section. The small-scale roughness is described by two functions $\eta_+(\varphi)$ and $\eta_-(\varphi)$, so that

$$h_\pm(\varphi) = f_\pm(\varphi)+\eta_\pm(\varphi). \tag{2}$$

Our purpose is to determine the ensemble averaged scattered field given an arbitrary incident field. In particular, we are interested in the volumetric effects and the influence of surface roughness.

The incident wave is taken as a horizontally polarized, two-dimensional plane shear wave, i.e. the displacement $\mathbf{u}(\mathbf{r}, t)$ is perpendicular to the plane of propagation, the $r\varphi$-plane of Fig. 1. We assume time harmonic conditions with an angular frequency ω. Suppressing a factor $\exp(-i\omega t)$ throughout we denote the incident, scattered and total displacement fields by $u^i(\mathbf{r})$, $u^s(\mathbf{r})$ and $u(\mathbf{r})$, respectively. Here, $u = u^i + u^s$. The elastodynamic equation of motion then reduces to Helmholtz' equation,

$$\nabla^2 u + k^2 u = 0. \tag{3}$$

Here the wave number $k = \omega/c$, where $c = \sqrt{\mu/\rho}$ is the speed of shear waves.

To solve the problem we use the null field approach following Boström *et al.* (1994) with some modifications to account for the fact that the surfaces C_+ and C_- do not coincide. The basic idea is to add a fictitious curve C_w as shown in Fig. 1. In this case C_w is taken to be a circular arc of radius a. Starting from eqn (3) we can easily derive the following integral representations:

$$u^i(\mathbf{r}') + \int_{C_+ + C_w} \left[u(\mathbf{r}) \frac{\partial G(\mathbf{r},\mathbf{r}')}{\partial n} - G(\mathbf{r},\mathbf{r}') \frac{\partial u(\mathbf{r})}{\partial n} \right] dC = \begin{cases} u(\mathbf{r}') & \mathbf{r}' \text{ outside } C_+ + C_w \\ 0 & \mathbf{r}' \text{ inside } C_+ + C_w \end{cases} \tag{4a}$$

$$-\int_{C_- + C_w} \left[u(\mathbf{r}) \frac{\partial G(\mathbf{r},\mathbf{r}')}{\partial n} - G(\mathbf{r},\mathbf{r}') \frac{\partial u(\mathbf{r})}{\partial n} \right] dC = \begin{cases} u(\mathbf{r}') & \mathbf{r}' \text{ inside } C_- + C_w \\ 0 & \mathbf{r}' \text{ outside } C_- + C_w \end{cases} \tag{4b}$$

where $G(\mathbf{r}, \mathbf{r}')$ is the free space Green function.

Utilizing the general solution to eqn (3) in polar coordinates we define two sets of basis functions. Firstly, we introduce a set of regular functions $\mathrm{Re}\,\chi_n = \frac{1}{2}J_n(kr)\,e^{in\varphi}$, where $J_n(kr)$ is the cylindrical Bessel function which has the property of being bounded at the origin. Secondly, we define a set of basis functions $\chi_n = \frac{1}{2}H_n(kr)\,e^{in\varphi}$ corresponding to outgoing waves. Here, $H_n(kr)$ is the cylindrical Hankel function of the first kind. The incident field u^i and the scattered field u^s can now be expanded as follows:

$$u^i = \sum_{n=-\infty}^{\infty} a_n \,\mathrm{Re}\,\chi_n \tag{5a}$$

$$u^s = \sum_{n=-\infty}^{\infty} f_n \chi_n. \tag{5b}$$

The expansion (5b) is valid everywhere outside the circumscribed circle of $C_+ + C_w$.

Expanding the free space Green function $G(\mathbf{r}, \mathbf{r}')$ we obtain

$$G(\mathbf{r},\mathbf{r}') = i\sum_n \mathrm{Re}\,\chi_n^*(\mathbf{r}_<)\chi_n(\mathbf{r}_>) = i\sum_n \mathrm{Re}\,\chi_n(\mathbf{r}_<)\chi_n^*(\mathbf{r}_>) \tag{6}$$

where $\mathrm{Re}\,\chi_n^* = \frac{1}{2}J_n(kr)\exp(-in\varphi)$ and $\chi_n^* = \frac{1}{2}H_n(kr)\exp(-in\varphi)$. If $r < r'$, then $\mathbf{r}_< = \mathbf{r}$ and $\mathbf{r}_> = \mathbf{r}'$ and otherwise the other way around.

Substituting into eqns (4) we obtain

$$f_n = i\int_{C_+ + C_w} \left(u \frac{\partial\,\mathrm{Re}\,\chi_n^*}{\partial n} - \mathrm{Re}\,\chi_n^* \frac{\partial u}{\partial n} \right) dC \tag{7a}$$

$$a_n = -i\int_{C_+ + C_w} \left(u \frac{\partial \chi_n^*}{\partial n} - \chi_n^* \frac{\partial u}{\partial n} \right) dC \tag{7b}$$

$$0 = i\int_{C_- + C_w} \left(u \frac{\partial\,\mathrm{Re}\,\chi_n^*}{\partial n} - \mathrm{Re}\,\chi_n^* \frac{\partial u}{\partial n} \right) dC. \tag{7c}$$

The displacement field on $C_- + C_w$ is expanded in regular basis functions,

$$u = \sum_n \alpha_n \operatorname{Re} \chi_n. \tag{8}$$

Following Boström and Olsson (1987) we introduce an auxiliary field $v(\varphi)$ in order to avoid the singularity of the traction at the crack tips:

$$v(\varphi) = \begin{cases} \dfrac{1}{Z(\varphi)}[u_+(\varphi) - u_-(\varphi)] & -\varphi_0 < \varphi < \varphi_0 \\ \dfrac{1}{kZ(\varphi)}\dfrac{\partial u}{\partial n} = \dfrac{1}{\mu k Z(\varphi)} t_w & \varphi_0 < \varphi < 2\pi - \varphi_0. \end{cases} \tag{9}$$

Here, u_+ and u_- are the displacement fields on C_+ and C_-, respectively, and t_w denotes the traction at the fictitious surface C_w. The function $Z(\varphi)$ is chosen so that $v(\varphi)$ is continuous. In the following section, where the surface roughness is considered, we assume that the tangents of C_+ and C_- coincide with the tangent of C_w at the crack tips. This assumption simplifies the conditions to be fulfilled at $\varphi = \pm\varphi_0$ considerably. Hence, the expression for $Z(\varphi)$ used by Boström *et al.* (1994) simplifies to

$$Z(\varphi) = \begin{cases} \sqrt{ka(\varphi_0^2 - \varphi^2)} & -\varphi_0 < \varphi < \varphi_0 \\ \dfrac{1}{2}\sqrt{\dfrac{\varphi_0(\pi - \varphi_0)}{ka(\varphi - \varphi_0)(2\pi - \varphi_0 - \varphi)}} & \varphi_0 < \varphi < 2\pi - \varphi_0. \end{cases} \tag{10}$$

It should be noted that $Z(\varphi)$ can always be multiplied by an arbitrary function of φ without affecting the continuity of $v(\varphi)$. Expanding $v(\varphi)$ in terms of trigonometric functions we obtain:

$$v(\varphi) = \sum_n \beta_n e^{in\varphi}. \tag{11}$$

Summing up we have the following boundary conditions:

$$\text{On } C_+: \quad u = \sum_n \alpha_n \operatorname{Re}\chi_n + Z\sum_n \beta_n e^{in\varphi} \qquad \frac{\partial u}{\partial n} = 0$$

$$\text{On } C_-: \quad u = \sum_n \alpha_n \operatorname{Re}\chi_n \qquad \frac{\partial u}{\partial n} = \sum_n \alpha_n \frac{\partial \operatorname{Re}\chi_n}{\partial n} = 0$$

$$\text{On } C_w: \quad u = \sum_n \alpha_n \operatorname{Re}\chi_n \qquad \frac{\partial u}{\partial n} = \sum_n \alpha_n \frac{\partial \operatorname{Re}\chi_n}{\partial n} = kZ\sum_n \beta_n e^{in\varphi}$$

where we have utilized that the traction is zero on C_+ and C_-.

Substituting into eqns (7) we obtain

$$f_n = i\sum_{n'} \alpha_{n'} \int_{C_- - C_w} \operatorname{Re}\chi_{n'} \frac{\partial \operatorname{Re}\chi_n^*}{\partial n} dC + i\sum_{n'} \beta_{n'} \int_{C_+} Z e^{in'\varphi} \frac{\partial \operatorname{Re}\chi_n^*}{\partial n} dC - ik\sum_{n'} \beta_{n'} \int_{C_w} Z e^{in'\varphi} \operatorname{Re}\chi_n^* dC \tag{12a}$$

$$a_n = \alpha_n - \mathrm{i}\sum_{n'} \alpha_{n'} \int_{C_-} \operatorname{Re}\chi_{n'} \frac{\partial \chi_n^*}{\partial n} \mathrm{d}C - \mathrm{i}\sum_{n'} \beta_{n'} \int_{C_+} Z\,\mathrm{e}^{\mathrm{i}n'\varphi} \frac{\partial \chi_n^*}{\partial n} \mathrm{d}C$$

$$+\mathrm{i}\sum_{n'} \alpha_{n'} \int_{C_-} \operatorname{Re}\chi_{n'} \frac{\partial \chi_n^*}{\partial n} \mathrm{d}C \qquad (12b)$$

$$0 = \mathrm{i}\sum_{n'} \alpha_{n'} \int_{C_- + C_w} \operatorname{Re}\chi_{n'} \frac{\partial \operatorname{Re}\chi_n^*}{\partial n} \mathrm{d}C - \mathrm{i}k\sum_{n'} \beta_{n'} \int_{C_w} Z\,\mathrm{e}^{\mathrm{i}n'\varphi} \operatorname{Re}\chi_n^* \mathrm{d}C \qquad (12c)$$

where eqn (12b) has been rewritten using a Betti identity. Equations (12) can be expressed in matrix notation as

$$\mathbf{f} = \mathrm{i}\mathbf{P}\boldsymbol{\alpha} + \mathrm{i}\operatorname{Re}\mathbf{R}\boldsymbol{\beta} - \mathrm{i}\mathbf{S}\boldsymbol{\beta} \qquad (13a)$$

$$\mathbf{a} = \boldsymbol{\alpha} - \mathrm{i}\mathbf{U}\boldsymbol{\alpha} - \mathrm{i}\mathbf{R}\boldsymbol{\beta} + \mathrm{i}\mathbf{V}\boldsymbol{\alpha} \qquad (13b)$$

$$0 = \mathbf{Q}\boldsymbol{\alpha} - \mathbf{S}\boldsymbol{\beta} \qquad (13c)$$

where $\mathbf{f}$, $\mathbf{a}$, $\boldsymbol{\alpha}$ and $\boldsymbol{\beta}$ are column vectors corresponding to the coefficients $f_n, \ldots, \beta_n$ and the elements of the matrices are defined as follows:

$$P_{nn'} = \int_{C_+ + C_w} \operatorname{Re}\chi_{n'} \frac{\partial \operatorname{Re}\chi_n^*}{\partial n} \mathrm{d}C \qquad (14a)$$

$$Q_{nn'} = \int_{C_- + C_w} \operatorname{Re}\chi_{n'} \frac{\partial \operatorname{Re}\chi_n^*}{\partial n} \mathrm{d}C \qquad (14b)$$

$$\operatorname{Re} R_{nn'} = \int_{C_+} Z\,\mathrm{e}^{\mathrm{i}n'\varphi} \frac{\partial \operatorname{Re}\chi_n^*}{\partial n} \mathrm{d}C \qquad (14c)$$

$$R_{nn'} = \int_{C_+} Z\,\mathrm{e}^{\mathrm{i}n'\varphi} \frac{\partial \chi_n^*}{\partial n} \mathrm{d}C \qquad (14d)$$

$$S_{nn'} = k\int_{C_w} Z\,\mathrm{e}^{\mathrm{i}n'\varphi} \operatorname{Re}\chi_n^* \mathrm{d}C \qquad (14e)$$

$$U_{nn'} = \int_{C_+} \operatorname{Re}\chi_{n'} \frac{\partial \chi_n^*}{\partial n} \mathrm{d}C \qquad (14f)$$

$$V_{nn'} = \int_{C_-} \operatorname{Re}\chi_{n'} \frac{\partial \chi_n^*}{\partial n} \mathrm{d}C. \qquad (14g)$$

Eliminating $\boldsymbol{\alpha}$ and $\boldsymbol{\beta}$ from eqns (13) we obtain a relation between the incident field and the scattered field:

$$\mathbf{f} = \mathbf{T}\mathbf{a} \qquad (15)$$

where

$$\mathbf{T} = \mathrm{i}(\mathbf{P}\mathbf{Q}^{-1}\mathbf{S} + \operatorname{Re}\mathbf{R} - \mathbf{S})\mathbf{W}^{-1} \qquad (16)$$

and

$$\mathbf{W} = (\mathbf{I} + \mathrm{i}\mathbf{V} - \mathrm{i}\mathbf{U})\mathbf{Q}^{-1}\mathbf{S} - \mathrm{i}\mathbf{R}. \qquad (17)$$

The $\mathbf{T}$ matrix (transition matrix) contains all relevant properties of the scatterer, i.e. given any incident field $\mathbf{a}$ it is possible to compute the scattered field $\mathbf{f}$.

For the case of deterministic curves, C_+ and C_-, the **T** matrix can be computed using eqns (16), (17) and (14). In the present case, however, the matrix elements of eqns (14) cannot be computed, except for $S_{nn'}$, due to the random behaviour of the surface roughness. Instead we proceed to compute an ensemble average of the scattered field. To do this we have to make some additional assumptions regarding the properties of the surfaces.

STATISTICAL DESCRIPTION OF THE SURFACES

According to eqn (2) the surfaces $C_\pm$ are described by the functions $h_\pm(\varphi) = f_\pm(\varphi) + \eta_\pm(\varphi)$, where $f_\pm(\varphi) = \langle h_\pm(\varphi)\rangle$ are ensemble averages. These can be prescribed more or less arbitrarily as long as the functions are nonnegative and approach zero at the crack tips. Here we have chosen the functions

$$f_\pm(\varphi) = \varepsilon a \cos^2 \frac{\pi\varphi}{2\varphi_0} \tag{18}$$

where $\varepsilon \ll 1$. In other words, $2\varepsilon a$ is the average gap width at the centre of the crack. This choice of $f_\pm(\varphi)$ has the advantage that the average of curves $C_\pm$ approach the fictitious surface C_w so that the slope is continuous, which simplifies the analysis considerably. In fact, our definition of the function $Z(\varphi)$, see eqn (10), assumes that not only the ensemble averages $f_\pm(\varphi) = \langle h_\pm(\varphi)\rangle$ but also the functions $h_\pm(\varphi)$ satisfy this condition.

Our purpose is to study an ensemble of rough scatterers with identical statistical properties in order to calculate the ensemble average of the scattered field $u^s = \Sigma f_n \chi_n = \Sigma T_{nn'} a_{n'} \chi_n$. The roughness is described by the functions $\eta_\pm(\varphi)$, where $\langle \eta_\pm(\varphi)\rangle = 0$. We assume that $\eta_\pm(\varphi)$ are continuously differentiable functions on the interval $-\varphi_0 \leqslant \varphi \leqslant \varphi_0$. It turns out that we need expressions for the ensemble averages of $\eta'_\pm(\varphi)$, $\eta_\pm(\varphi)\eta_\pm(\varphi')$, $\eta'_\pm(\varphi)\eta_\pm(\varphi')$ and $\eta'_\pm(\varphi)\eta'_\pm(\varphi')$. Furthermore, we need expressions for $\langle \eta_+(\varphi)\eta_-(\varphi')\rangle$ and its derivatives.

It is easily seen that $\langle \eta'_\pm(\varphi)\rangle = 0$. For the correlation functions $\langle \eta_\pm(\varphi)\eta_\pm(\varphi')\rangle$ we have to make some assumptions. Several models have been proposed [see Ogilvy (1991) for a detailed review of the literature]. In most cases a stationary model is used meaning that any statistical properties involving two points on the surface depend only on the relative positions of these points, i.e. $\langle \eta_\pm(\varphi)\eta_\pm(\varphi')\rangle = g_\pm(\varphi-\varphi')$, where $g_\pm(\varphi-\varphi')$ are some suitably chosen functions, e.g. $g_\pm(\varphi-\varphi') \propto \exp[-a^2(\varphi-\varphi')^2/2\lambda_c^2]$. Here, λ_c is a correlation length which is related to the average distance between two consecutive peaks on the surface. However, in the present case the stationary model has the unpleasant property that $\langle [r(\pm\varphi_0)-a]^2\rangle \neq 0$, i.e. that the curves C_+ and C_- may be overlapping in the neighbourhood of the crack tips. To avoid this difficulty we prescribe a nonstationary roughness such that

$$\langle \eta_\pm(\varphi)\eta_\pm(\varphi')\rangle = \sigma^2 a^2 \cos^2 \frac{\pi\varphi}{2\varphi_0} \cos^2 \frac{\pi\varphi'}{2\varphi_0} \exp\left\{-\frac{a^2}{\lambda_c^2}[1-\cos(\varphi-\varphi')]\right\} \tag{19}$$

where σ can be interpreted as a local RMS value of the height of the irregularities. Since we only consider slightly rough surfaces we assume that $\sigma \ll 1$. Obviously, $\langle h_\pm(\pm\varphi_0)^2\rangle = \langle \eta_\pm(\pm\varphi_0)^2\rangle = 0$ and, consequently, $\langle [r(\pm\varphi_0)-a]^2\rangle = 0$ or $r(\pm\varphi_0) = a$, as desired. Furthermore, $r'(\pm\varphi_0) = 0$, i.e. the tangents of C_+ and C_- coincide with the tangent of C_w at the crack tips for each individual crack of the ensemble. This property has already been utilized when the function $Z(\varphi)$ was defined, see eqn (10).

The main reason for choosing the factor $\exp\{(-a^2/\lambda_c^2)[1-\cos(\varphi-\varphi')]\}$ in eqn (19), rather than the ordinary Gaussian correlation function, is that it is periodic on the interval $[0, 2\pi]$. Thus it can be expanded in a Fourier series in a very attractive way:

$$\exp\left\{-\frac{a^2}{\lambda_c^2}[1-\cos(\varphi-\varphi')]\right\} = \sum_n \xi_n \mathrm{e}^{\mathrm{i}n(\varphi-\varphi')} \tag{20}$$

where the coefficients ξ_n are given by

$$\xi_n = \mathrm{I}_n(a^2/\lambda_c^2)\exp(-a^2/\lambda_c^2). \tag{21}$$

Here, $\mathrm{I}_n(x) = \mathrm{i}^{-n}\mathrm{J}_n(x)$ is a modified Bessel function of the first kind.

It should also be noted that there is no significant numerical difference between the Gaussian and the periodic correlation functions for the values of λ_c/a that are considered here.

The expressions for $\langle\eta'_\pm(\varphi)\eta_\pm(\varphi')\rangle$, $\langle\eta_\pm(\varphi)\eta'_\pm(\varphi')\rangle$ and $\langle\eta'_\pm(\varphi)\eta'_\pm(\varphi')\rangle$ are obtained from eqn (19) by differentiation.

The proposed correlation function, eqn (19), implies that both surfaces have identical statistical properties, in particular the same values of σ and λ_c. There is no fundamental difficulty involved in handling two surfaces with different values of σ and/or λ_c, but the calculations will become considerably lengthier and much more cumbersome to carry out. Since there does not seem to be any physical justification for taking this possibility into account we have refrained from doing so.

We also assume that $\langle\eta_+(\varphi)\eta_-(\varphi')\rangle \equiv 0$, i.e. the surfaces are totally uncorrelated. This is an assumption that is open to criticism. It is reasonable to believe that the kind of mechanism that has created the crack determines to what extent the surfaces are correlated. It can be shown that the extreme case where $\langle\eta_+(\varphi)\eta_-(\varphi')\rangle = \langle\eta_\pm(\varphi)\eta_\pm(\varphi')\rangle$ leads to analytical results that are rather similar to those obtained for the uncorrelated case. However, no numerical results are presented here.

If the surfaces are completely uncorrelated we have to require that $h_\pm(\varphi) = f_\pm(\varphi)\pm\eta_\pm(\varphi) \geqslant 0$ for each individual crack to make sure that the curves C_+ and C_- do not overlap. This can only be true if $\sigma \leqslant \varepsilon$.

ENSEMBLE AVERAGED T MATRIX AND THE SCATTERED FIELD

To determine the ensemble averaged **T** matrix and the corresponding scattered field we replace r by $a\pm h_\pm(\varphi)$ on C_+ and C_- in eqns (14). Expanding all matrix elements in powers of $h_\pm(\varphi)/a$ and $h'_\pm(\varphi)/a$ and substituting into eqn (16) we obtain a series expansion of the **T** matrix for each individual crack of the ensemble. Taking the ensemble average and utilizing eqns (2), (18) and (19), and similar series expansions for $\langle\eta'_\pm(\varphi)\eta_\pm(\varphi')\rangle$, $\langle\eta_\pm(\varphi)\eta'_\pm(\varphi')\rangle$ and $\langle\eta'_\pm\varphi)\eta'_\pm(\varphi')\rangle$, we obtain after some rather tedious calculations the ensemble averaged T matrix on the following form:

$$\langle\mathbf{T}\rangle = \mathbf{T}_0+\varepsilon\mathbf{T}_1+\varepsilon^2\mathbf{T}_{20}+\sigma^2\mathbf{T}_2+\dots. \tag{22}$$

Here,

$$\mathbf{T}_0 = \mathrm{i}\,\mathrm{Re}\,\mathbf{R}_0\mathbf{W}_0^{-1} \tag{23a}$$

$$\mathbf{T}_1 = [(2\mathrm{i}\mathbf{P}_1^0\mathbf{Q}_0^{-1}\mathbf{S}-2\,\mathrm{Re}\,\mathbf{R}_0\mathbf{W}_0^{-1}\mathbf{U}_1^0-\mathrm{i}\,\mathrm{Re}\,\mathbf{R}_0\mathbf{W}_0^{-1}\mathbf{Q}_0^{-1}\mathbf{P}_1^0)\mathbf{Q}_0^{-1}\mathbf{S}+\mathrm{i}\,\mathrm{Re}\,\mathbf{R}_1^0 \\ -\mathrm{Re}\,\mathbf{R}_0\mathbf{W}_0^{-1}\mathbf{R}_1^0]\mathbf{W}_0^{-1} \tag{23b}$$

$$\begin{aligned}\mathbf{T}_{20} = \{[&2\mathrm{i}\mathbf{P}_1^0\mathbf{Q}_0^{-1}\mathbf{P}_1^0-4\mathbf{P}_1^0\mathbf{Q}_0^{-1}\mathbf{S}\mathbf{W}_0^{-1}\mathbf{U}_1^0-2\mathrm{i}\mathbf{P}_1^0\mathbf{Q}_0^{-1}\mathbf{S}\mathbf{W}_0^{-1}\mathbf{Q}_0^{-1}\mathbf{P}_1^0 \\ &-2\,\mathrm{Re}\,\mathbf{R}_1^0\mathbf{W}_0^{-1}\mathbf{U}_1^0-\mathrm{i}\,\mathrm{Re}\,\mathbf{R}_1^0\mathbf{W}_0^{-1}\mathbf{Q}_0^{-1}\mathbf{P}_1^0+\mathrm{Re}\,\mathbf{R}_0\mathbf{W}_0^{-1}(-4\mathrm{i}\mathbf{U}_1^0\mathbf{Q}_0^{-1}\mathbf{S}\mathbf{W}_0^{-1}\mathbf{U}_1^0 \\ &+2\mathbf{U}_1^0\mathbf{Q}_0^{-1}\mathbf{S}\mathbf{W}_0^{-1}\mathbf{Q}_0^{-1}\mathbf{P}_1^0+2\mathbf{Q}_0^{-1}\mathbf{P}_1^0\mathbf{Q}_0^{-1}\mathbf{S}\mathbf{W}_0^{-1}\mathbf{U}_1^0+\mathrm{i}\mathbf{Q}_0^{-1}\mathbf{P}_1^0\mathbf{Q}_0^{-1}\mathbf{S}\mathbf{W}_0^{-1}\mathbf{Q}_0^{-1}\mathbf{P}_1^0 \\ &-2\mathrm{i}\mathbf{R}_1^0\mathbf{W}_0^{-1}\mathbf{U}_1^0+\mathbf{R}_1^0\mathbf{W}_0^{-1}\mathbf{Q}_0^{-1}\mathbf{P}_1^0-2\mathbf{U}_1^0\mathbf{Q}_0^{-1}\mathbf{P}_1^0-\mathrm{i}\mathbf{Q}_0^{-1}\mathbf{P}_1^0\mathbf{Q}_0^{-1}\mathbf{P}_1^0)]\mathbf{Q}_0^{-1}\mathbf{S} \\ &-2\mathbf{P}_1^0\mathbf{Q}_0^{-1}\mathbf{S}\mathbf{W}_0^{-1}\mathbf{R}_1^0-\mathrm{Re}\,\mathbf{R}_1^0\mathbf{W}_0^{-1}\mathbf{R}_1^0+\mathrm{i}\,\mathrm{Re}\,\mathbf{R}_2\end{aligned}$$

$$+\operatorname{Re}\mathbf{R}_0\mathbf{W}_0^{-1}(-2\mathrm{i}\mathbf{U}_1^0\mathbf{Q}_0^{-1}\mathbf{S}\mathbf{W}_0^{-1}\mathbf{R}_1^0+\mathbf{Q}_0^{-1}\mathbf{P}_1^0\mathbf{Q}_0^{-1}\mathbf{S}\mathbf{W}_0^{-1}\mathbf{R}_1^0-\mathrm{i}\mathbf{R}_1^0\mathbf{W}_0^{-1}\mathbf{R}_1^0$$
$$+\mathrm{i}\mathbf{Q}_0^{-1}\mathbf{P}_2\mathbf{Q}_0^{-1}\mathbf{S}-\mathbf{R}_2)\}\mathbf{W}_0^{-1} \tag{23c}$$

$$\mathbf{T}_2=\Bigg(\sum_m \xi_m\{[\mathrm{i}\mathbf{P}_1^m\mathbf{Q}_0^{-1}\mathbf{P}_1^{-m}-2\mathbf{P}_1^m\mathbf{Q}_0^{-1}\mathbf{S}\mathbf{W}_0^{-1}\mathbf{U}_1^{-m}-\mathrm{i}\mathbf{P}_1^m\mathbf{Q}_0^{-1}\mathbf{S}\mathbf{W}_0^{-1}\mathbf{Q}_0^{-1}\mathbf{P}_1^{-m}$$
$$-\operatorname{Re}\mathbf{R}_1^m\mathbf{W}_0^{-1}\mathbf{U}_1^{-m}+\operatorname{Re}\mathbf{R}_0\mathbf{W}_0^{-1}(-2\mathrm{i}\mathbf{U}_1^m\mathbf{Q}_0^{-1}\mathbf{S}\mathbf{W}_0^{-1}\mathbf{U}_1^{-m}$$
$$+\mathbf{U}_1^m\mathbf{Q}_0^{-1}\mathbf{S}\mathbf{W}_0^{-1}\mathbf{Q}_0^{-1}\mathbf{P}_1^{-m}+\mathbf{Q}_0^{-1}\mathbf{P}_1^m\mathbf{Q}_0^{-1}\mathbf{S}\mathbf{W}_0^{-1}\mathbf{U}_1^{-m}+\mathrm{i}\mathbf{Q}_0^{-1}\mathbf{P}_1^m\mathbf{Q}_0^{-1}\mathbf{S}\mathbf{W}_0^{-1}\mathbf{Q}_0^{-1}\mathbf{P}_1^{-m}$$
$$-\mathrm{i}\mathbf{R}_1^m\mathbf{W}_0^{-1}\mathbf{U}_1^{-m}-\mathbf{U}_1^m\mathbf{Q}_0^{-1}\mathbf{P}_1^{-m}-\mathrm{i}\mathbf{Q}_0^{-1}\mathbf{P}_1^m\mathbf{Q}_0^{-1}\mathbf{P}_1^{-m})]\mathbf{Q}_0^{-1}\mathbf{S}$$
$$-\mathbf{P}_1^m\mathbf{Q}_0^{-1}\mathbf{S}\mathbf{W}_0^{-1}\mathbf{R}_1^{-m}-\operatorname{Re}\mathbf{R}_1^m\mathbf{W}_0^{-1}\mathbf{R}_1^{-m}$$
$$+\operatorname{Re}\mathbf{R}_0\mathbf{W}_0^{-1}(-\mathrm{i}\mathbf{U}_1^m\mathbf{Q}_0^{-1}\mathbf{S}\mathbf{W}_0^{-1}\mathbf{R}_1^{-m}-\mathrm{i}\mathbf{R}_1^m\mathbf{W}_0^{-1}\mathbf{R}_1^{-m})\}$$
$$+\mathrm{i}\operatorname{Re}\mathbf{R}_2+\operatorname{Re}\mathbf{R}_0\mathbf{W}_0^{-1}(\mathrm{i}\mathbf{Q}_0^{-1}\mathbf{P}_2\mathbf{Q}_0^{-1}\mathbf{S}-\mathbf{R}_2)\Bigg)\mathbf{W}_0^{-1} \tag{23d}$$

and

$$\mathbf{W}_0=\mathbf{Q}_0^{-1}\mathbf{S}-\mathrm{i}\mathbf{R}_0.$$

The explicit expressions for the matrices in eqns (23) are given in the appendix.

To calculate the scattered field we note that $u^s=\Sigma T_{nn'}a_{n'}\chi_n$ according to eqns (5b) and (15). Here a_n are the expansion coefficients of the incident field u^i, see eqn (5a). In the case of an incident plane wave of amplitude u_0 and angle of incidence α as defined in Fig. 1 we have $a_n=2u_0\mathrm{i}^n\mathrm{e}^{-\mathrm{i}n\alpha}$. Thus, $u^s=u_0\Sigma T_{nn'}\mathrm{i}^{n'}\mathrm{H}_n(kr)\,\mathrm{e}^{\mathrm{i}(n\varphi-n'\alpha)}$. The far field is obtained by replacing $\mathrm{H}_n(kr)$ by its asymptotic expression $(2/\pi kr)^{1/2}\exp[\mathrm{i}(kr-n\pi/2-\pi/4)]$. The result is that the scattered field is obtained as a series expansion:

$$u^s=u_0\frac{\mathrm{e}^{\mathrm{i}kr}}{(kr)^{1/2}}\bar{u}^s(\varphi)$$

where

$$\bar{u}^s(\varphi)=\frac{1-\mathrm{i}}{\pi^{1/2}}\sum_{nn'}\mathrm{i}^{n'-n}[(\mathbf{T}_0)_{nn'}+\varepsilon(\mathbf{T}_1)_{nn'}+\varepsilon^2(\mathbf{T}_{20})_{nn'}+\sigma^2(\mathbf{T}_2)_{nn'}+\ldots]\,\mathrm{e}^{\mathrm{i}(n\varphi-n'\alpha)} \tag{24}$$

is a dimensionless far field amplitude.

NUMERICAL RESULTS

The scattered field far away from the crack is calculated numerically from eqn (24) using eqns (23) and the matrix elements from the appendix. Results are obtained for various values of the frequency, the angle of incidence, the average central gap width 2ε, the RMS height σ and the correlation length λ_c. In all cases the central angle of the crack $2\varphi_0$ is taken to be 60°.

In Figs 2(a–c) the magnitude of the far field amplitude, as defined in eqn (24), is plotted against the scattering angle for three different frequencies, $ka=1$, 5 and 10, respectively, and for various values of ε, σ and λ_c. The angle of incidence is $\alpha=90°$ in all cases. In Figs 3(a–c) the corresponding results for $\alpha=45°$ are shown. The back-scattered field is obtained by taking $\varphi=\alpha+\pi$ in eqn (24). Some results are shown in Figs 4(a–c). Where the effects of roughness are hardly visible we have chosen to show the volumetric effects only.

One obvious conclusion is that the effects of roughness in general are small compared to the volumetric effects. These, on the other hand, can be of considerable importance,

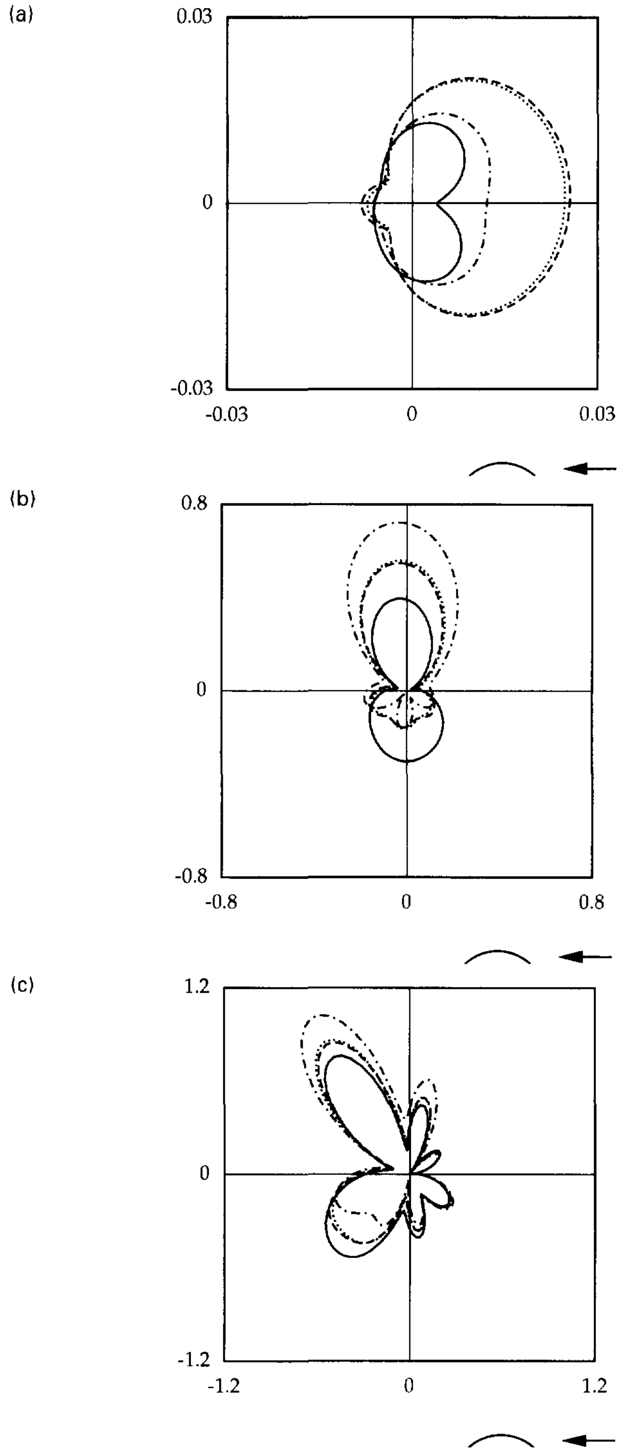

Fig. 2. (a) Polar plot of the scattered far field amplitude versus the scattering angle for $\alpha = 90^{\circ}$, $ka = 1$, $\lambda_c/a = 0.1$, and for $\varepsilon = \sigma = 0$ (——), $\varepsilon = 0.02$, $\sigma = 0$ (-·-·-), $\varepsilon = 0.05$, $\sigma = 0$ (······), $\varepsilon = \sigma = 0.05$ (----). (b) Polar plot of the scattered far field amplitude versus the scattering angle for $\alpha = 90^{\circ}$, $ka = 5$, $\lambda_c/a = 0.1$, and for $\varepsilon = \sigma = 0$ (——), $\varepsilon = 0.05$, $\sigma = 0$ (······), $\varepsilon = \sigma = 0.05$ (----), $\varepsilon = 0.1$, $\sigma = 0$ (-·-·-). (c) Polar plot of the scattered far field amplitude versus the scattering angle for $\alpha = 90^{\circ}$, $ka = 10$, $\lambda_c/a = 0.05$, and for $\varepsilon = \sigma = 0$ (——), $\varepsilon = 0.02$, $\sigma = 0$ (······), $\varepsilon = \sigma = 0.02$ (----), $\varepsilon = 0.05$, $\sigma = 0$ (-·-·-).

especially for certain angles of incidence. In Figs 2 and 4 it is also possible to study the effects of overall curvature, which is responsible for the asymmetries with respect to the horizontal axis. According to Ogilvy (1991) the effect of nonplanar reference surfaces are among the unsolved questions of scattering from rough surfaces.

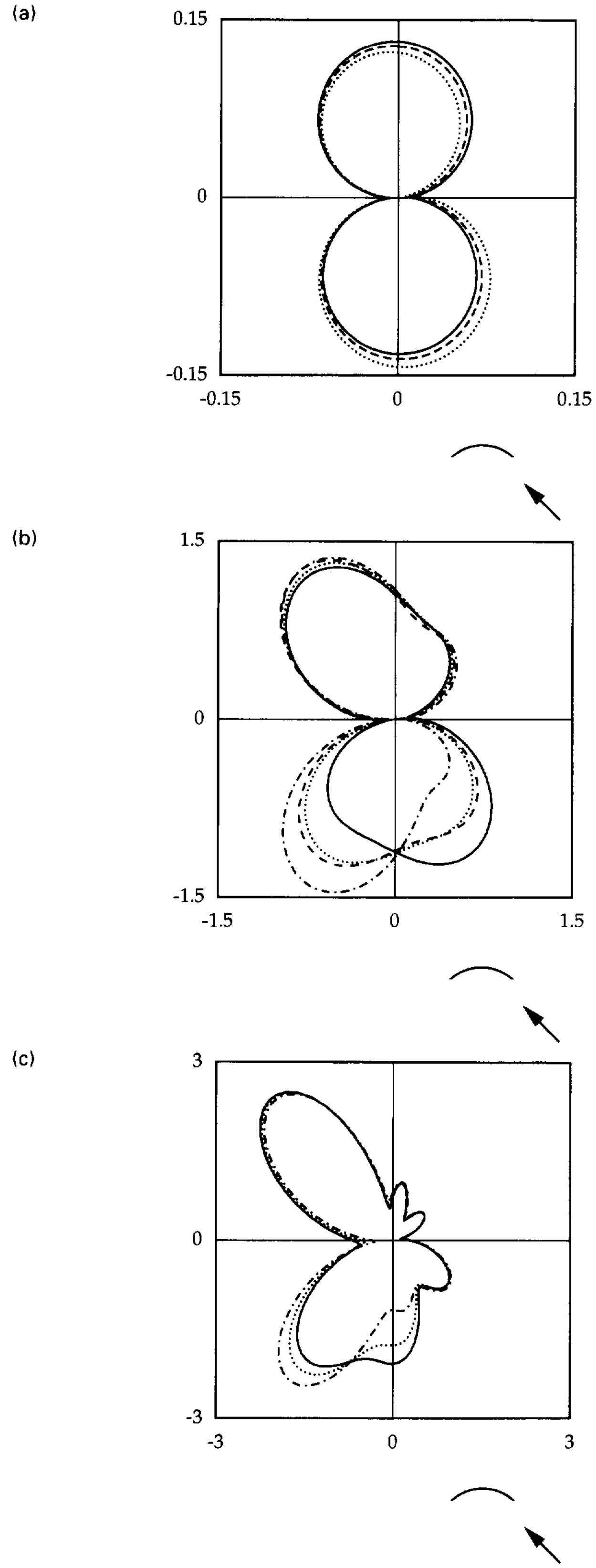

Fig. 3. (a) Polar plot of the scattered far field amplitude versus the scattering angle for $\alpha = 45^{\circ}$, $ka = 1$, and for $\varepsilon = \sigma = 0$ (——), $\varepsilon = 0.02$, $\sigma = 0$ (······), $\varepsilon = 0.05$, $\sigma = 0$ (----). (b) Polar plot of the scattered far field amplitude versus the scattering angle for $\alpha = 45^{\circ}$, $ka = 5$, $\lambda_c/a = 0.1$, and for $\varepsilon = \sigma = 0$ (——), $\varepsilon = 0.05$, $\sigma = 0$ (······), $\varepsilon = \sigma = 0.05$ (----), $\varepsilon = 0.1$, $\sigma = 0$ (-·-·-). (c) Polar plot of the scattered far field amplitude versus the scattering angle for $\alpha = 45^{\circ}$, $ka = 10$, and for $\varepsilon = \sigma = 0$ (——), $\varepsilon = 0.02$, $\sigma = 0$ (······), $\varepsilon = 0.05$, $\sigma = 0$ (-·-·-).

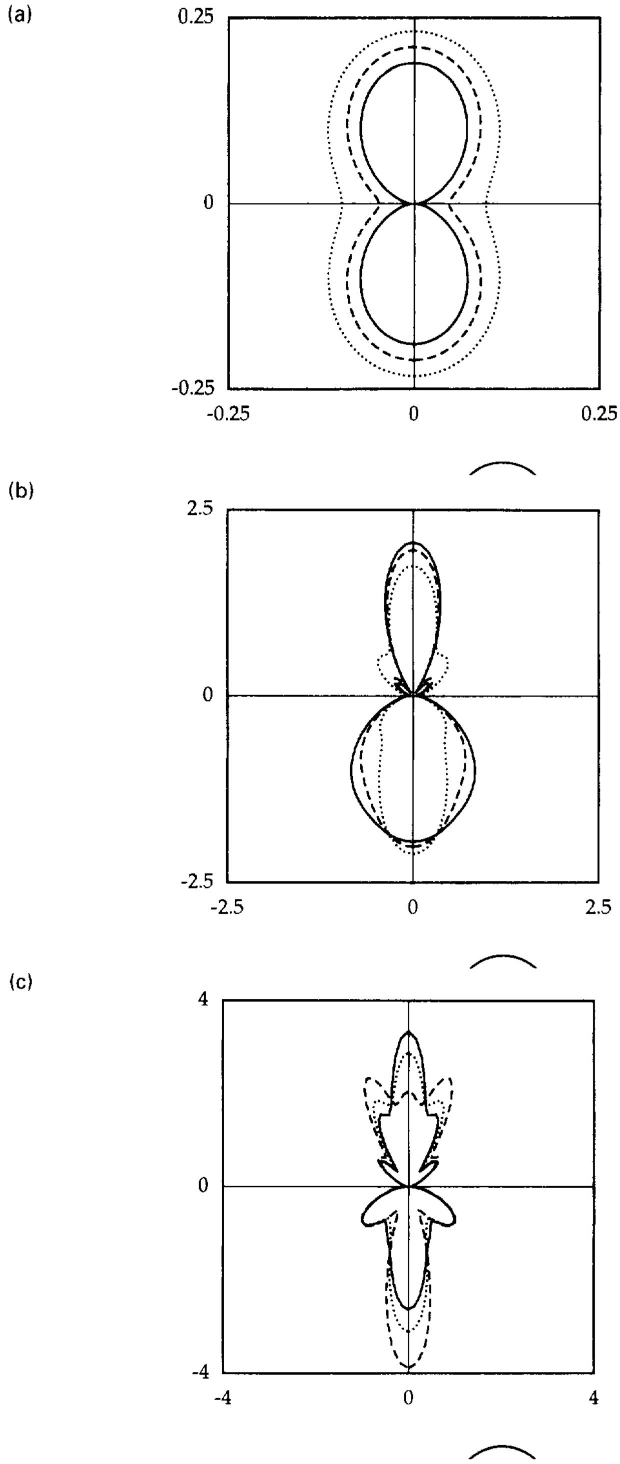

Fig. 4. (a) Polar plot of the back-scattered far field amplitude versus the angle of incidence for $ka = 1$, and for $\varepsilon = \sigma = 0$ (——), $\varepsilon = 0.1$, $\sigma = 0$ (······), $\varepsilon = 0.2$, $\sigma = 0$ (----). (b) Polar plot of the back-scattered far field amplitude versus the angle of incidence for $ka = 5$, and for $\varepsilon = \sigma = 0$ (——), $\varepsilon = 0.04$, $\sigma = 0$ (······), $\varepsilon = 0.1$, $\sigma = 0$ (----). (c) Polar plot of the back-scattered far field amplitude versus the angle of incidence for $ka = 10$, and for $\varepsilon = \sigma = 0$ (——), $\varepsilon = 0.02$, $\sigma = 0$ (······), $\varepsilon = 0.05$, $\sigma = 0$ (----).

The results are valid only as long as certain parameters are small. When the matrix elements of eqns (14) are calculated, $J_n(kr)$ and $H_n(kr)$ are expanded in Taylor series around $r = a$. Hence, $kah_{\pm}$ must be small, i.e. the condition $\varepsilon + \sigma \ll 1/ka$ must be fulfilled. This means that the deviation from the circular arc must be small compared to the wavelength.

Furthermore, the RMS height must be small compared to the correlation length, i.e. $\sigma \ll \lambda_c$. This restriction is less obvious from the analysis but is well-known from the literature, see Ogilvy (1991). A numerical check on this condition was performed by Jansson (1993) by calculating fourth-order elements of the **T** matrix. For obvious reasons no such attempt has been made here.

In the numerical results presented above we have a rather liberal view on the meaning of the term "small". The main reason for this is that the effect of roughness is hardly noticeable otherwise. Even if the results are not quantitatively correct they are believed to predict the tendency when the values of the so-called small parameters ε and σ are increased.

The matrices $\mathbf{T}_0$, $\mathbf{T}_1$ and $\mathbf{T}_{20}$ have been checked for symmetry and hermiticity. The symmetry condition follows from the fact that the system must be invariant under a change of direction of time, while hermiticity is a consequence of energy conservation. The conditions that must be fulfilled are

$$T_{n'n} = (-1)^{n+n'} T_{-n,-n'} \tag{25}$$

$$\mathbf{T} + \mathbf{T}^* + 2\mathbf{T}^*\mathbf{T} = 0. \tag{26}$$

Expanding eqns (25) and (26) in powers of ε we obtain conditions that can be used for a numerical check of $\mathbf{T}_0$, $\mathbf{T}_1$ and $\mathbf{T}_{20}$. However, the hermiticity condition can only be used for the deterministic part of the **T** matrix since the ensemble average of the nonlinear term $2\mathbf{T}^*\mathbf{T}$ is never calculated. In fact, we do not even calculate the ensembled averaged matrix $\mathbf{T}_2$ due to the storage problem caused by the matrices with three indices, e.g. $\mathbf{P}_1^m$. Instead we calculate $\mathbf{T}_2\mathbf{a}$ immediately.

In all cases the indices n and m of eqns (23d) and (24) run from -80 to 80 and from -40 to 40, respectively, to ensure convergence. The symmetry and hermiticity tests indicate that $n_{\max} = 80$ is more than sufficient. Increasing $m_{\max}$ above 40 does not result in any significant change.

CONCLUDING REMARKS

In the present paper the scattering from a rough volumetric crack is studied by the use of an analytical ensemble averaging technique. Obviously, the effect of roughness is more or less negligible compared to the volumetric effect. This observation is not particularly surprising considering the fact that the latter effect is of first order while roughness is a second-order effect as long as only ensemble averages are considered. Roughness may, of course, have a significant effect on the scattering properties of an individual crack of the ensemble. With the present method, however, it is not possible to make any predictions of these. Since the response from one specific crack is of interest in ultrasonic testing rather than an ensemble average of the response from several cracks, it seems reasonable to suggest a different approach to the study of scattering from cracks. One possible way could be to generate a number of randomly rough surfaces with equal statistical properties by some kind of numerical simulation and study the scattered field from each individual crack, for instance by using the method of the present work. Jansson (1995) has modelled a rough penny-shaped crack as a superposition of a finite number of doubly corrugated surfaces which are randomly translated and rotated with respect to each other. It seems likely that a similar model in combination with the approach of the present paper will give useful results.

Despite the above objection to the practical usefulness of the quantitative results presented here, the method should be useful in studying the influence of properties like roughness and the shape of the reference surfaces. At least in principle, it should be possible to replace the circular arc by another curve. There are certain restrictions to the null field approach, however, and in any case it will probably not be possible to reach this far by analytical calculations. Even if the circular arc is retained we can study different shapes of the reference surfaces by choosing another function $f(\varphi)$ in eqn (18). This may lead to more complicated computations, for instance it may be necessary to calculate the matrix elements of eqns (A1d–h) by numerical integration, but otherwise the procedure should be straightforward. The correlation function defined in eqn (19) may be changed, for instance by replacing the (almost) Gaussian factor by any of the various correlation functions that have been suggested [see Ogilvy (1991)]. This is equivalent to changing the coefficients ξ_m of eqn (21).

There are several other possible extensions of the present work. The possibility of studying a number of simulated deterministic surfaces, thus taking first-order roughness effects into account, has already been mentioned. Other possibilities include the scattering of P and SV waves, i.e. compressional waves and shear waves polarized in the plane of propagation, and the three-dimensional problem, of course. However, the analytical and numerical effort required in the three-dimensional case will most likely be of a completely different dimension.

Acknowledgements—The author wishes to thank Professor Anders Boström for valuable discussions during the progress of the present work. This project was financially supported by the Swedish Research Council for Engineering Sciences, and this is also gratefully acknowledged.

REFERENCES

Boström, A. and Olsson, P. (1987). Scattering of elastic waves by non-planar cracks. *Wave Motion* **9**, 61–76.

Boström, A., Jansson, P.-Å. and Olsson, P. (1994). Antiplane elastic wave scattering from a curved randomly rough crack. *J. Appl. Mech.* **61**, 835–842.

Jansson, P.-Å. (1993). Acoustic scattering from a rough sphere. *J. Acoust. Soc. Am.* **93**, 3032–3042.

Jansson, P.-Å. (1995). Elastic wave scattering from a rough penny-shaped crack. *Communications from Division of Mechanics*, 1995: 2, Chalmers University of Technology.

Lewis, P. A. (1990). Scattering of elastic waves by rough cracks. In *Elastic Waves and Ultrasonic Nondestructive Evaluation* (Edited by S. K. Datta, J. D. Achenbach and Y. S. Rajakapse). North-Holland, Amsterdam.

Ogilvy, J. A. (1991). *Theory of Wave Scattering from Random Rough Surfaces*. Adam Hilger, Bristol.

Ogilvy, J. A. and Culverwell, I. D. (1991). Elastic model for simulating ultrasonic inspection of smooth and rough defects. *Ultrasonics* **29**, 490–496.

Pao, Y.-H. and Varatharajulu, V. (1976). Scattering matrix for elastic waves. I. Theory. *J. Acoust. Soc. Am.* **60**, 556–566.

Waterman, P. C. (1965). Matrix formulation of electromagnetic scattering. *Proc. IEEE* **53**, 805–812.

Waterman, P. C. (1969). New formulation of acoustic scattering. *J. Acoust. Soc. Am.* **45**, 1417–1429.

Waterman, P. C. (1976). Matrix theory of elastic wave scattering. *J. Acoust. Soc. Am.* **60**, 567–580.

Waterman, P. C. (1978). Matrix theory of elastic wave scattering. II. A new conservation law. *J. Acoust. Soc. Am.* **63**, 1320–1325.

Zheng, W. and Ström, S. (1989). The null field approach to electromagnetic scattering from composite objects: the case of concavo-convex constituents. *IEEE Trans. Antennas Propagat.* **37**, 373–383.

APPENDIX

In eqns (23) the T matrix is expressed in terms of various matrices, the elements of which are given here.

$$[\mathbf{Q}_0^{-1}]_{nn'} = [2/\pi ka \mathrm{J}_n(ka)\mathrm{J}'_n(ka)]\delta_{nn'} \tag{A1a}$$

$$[\mathbf{R}_0]_{nn'} = \begin{cases} \dfrac{\pi}{2}\varphi_0 (ka)^{3/2}\mathrm{H}'_n(ka)\dfrac{\mathrm{J}_1[(n'-n)\varphi_0]}{n'-n} & n \neq n' \\ \dfrac{\pi}{4}\varphi_0^2 (ka)^{3/2}\mathrm{H}'_n(ka) & n = n' \end{cases} \tag{A1b}$$

$$[\mathbf{S}]_{nn'} = \frac{\pi}{4}\sqrt{ka\varphi_0(\pi-\varphi_0)}(-1)^{n'-n}\mathrm{J}_n(ka)\mathrm{J}_0[(n'-n)(\pi-\varphi_0)] \tag{A1c}$$

$$[\mathbf{P}_1^m]_{nn'} = p_{nn'}F_1(n'-n+m) \tag{A1d}$$

$$[\mathbf{R}_1^m]_{nn'} = (r_n - ms_n)F_2(n'-n+m) - \frac{\pi}{\varphi_0}s_n F_3(n'-n+m) \tag{A1e}$$

$$[\mathbf{U}_1^m]_{nn'} = u_{nn'}F_1(n'-n+m) \tag{A1f}$$

$$\begin{aligned}[\mathbf{P}_2]_{nn'} = {} & \tfrac{1}{8}(ka)^2\{ka\mathrm{J}'''_n(ka)\mathrm{J}_{n'}(ka) + 2\mathrm{J}''_n(ka)[\mathrm{J}_{n'}(ka) + ka\mathrm{J}'_{n'}(ka)] + \mathrm{J}'_n(ka)[2\mathrm{J}'_{n'}(ka) + ka\mathrm{J}''_{n'}(ka)]\}F_4(n'-n) \\ & + \frac{n\pi}{4\varphi_0}\{\mathrm{J}_n(ka)[\mathrm{J}_{n'}(ka) - ka\mathrm{J}'_{n'}(ka)] - ka\mathrm{J}'_n(ka)\mathrm{J}_{n'}(ka)\}F_5(n'-n)\end{aligned} \tag{A1g}$$

$$[\mathbf{R}_2]_{nn'} = \tfrac{1}{4}(ka)^{5/2}[ka\mathrm{H}'''_n(ka) + 2\mathrm{H}''_n(ka)]F_6(n'-n) - \frac{\pi}{2\varphi_0}(ka)^{1/2}n[ka\mathrm{H}'_n(ka) - \mathrm{H}_n(ka)]F_7(n'-n) \tag{A1h}$$

where

$$p_{nn'} = \tfrac{1}{4}\{ka[ka\mathrm{J}''_n(ka)\mathrm{J}_{n'}(ka)+\mathrm{J}'_n(ka)\mathrm{J}_{n'}(ka)+ka\mathrm{J}'_n(ka)\mathrm{J}'_{n'}(ka)]+n(n'-n)\mathrm{J}_n(ka)\mathrm{J}_{n'}(ka)\}$$

$$r_n = \tfrac{1}{2}(ka)^{3/2}[ka\mathrm{H}''_n(ka)+\mathrm{H}'_n(ka)]$$

$$s_n = \tfrac{1}{2}(ka)^{1/2}n\mathrm{H}_n(ka)$$

$$u_{nn'} = \tfrac{1}{4}\{ka[ka\mathrm{H}''_n(ka)\mathrm{J}_{n'}(ka)+\mathrm{H}'_n(ka)\mathrm{J}_{n'}(ka)+ka\mathrm{H}'_n(ka)\mathrm{J}'_{n'}(ka)]+n(n'-n)\mathrm{H}_n(ka)\mathrm{J}_{n'}(ka)\}$$

and

$$F_1(n) = \frac{\pi^2\sin(n\varphi_0)}{n(\pi^2-n^2\varphi_0^2)} \quad n\neq 0, n\neq \pm\pi/\varphi_0$$

$$F_1(0) = \varphi_0$$

$$F_1(\pm\pi/\varphi_0) = \varphi_0/2$$

$$F_2(n) = \frac{\pi}{4}\varphi_0\left[\frac{2\mathrm{J}_1(n\varphi_0)}{n}+\varphi_0\frac{\mathrm{J}_1(\pi-n\varphi_0)}{\pi-n\varphi_0}+\varphi_0\frac{\mathrm{J}_1(\pi+n\varphi_0)}{\pi+n\varphi_0}\right] \quad n\neq 0, n\neq\pm\pi/\varphi_0$$

$$F_2(0) = \frac{\pi}{4}\varphi_0^2+\tfrac{1}{2}\varphi_0^2\mathrm{J}_1(\pi)$$

$$F_2(\pm\pi/\varphi_0) = \frac{\varphi_0^2}{8}[4\mathrm{J}_1(\pi)+\pi+\mathrm{J}_1(2\pi)]$$

$$F_3(n) = \frac{\pi}{4}\varphi_0^2\left[\frac{\mathrm{J}_1(\pi+n\varphi_0)}{\pi+n\varphi_0}-\frac{\mathrm{J}_1(\pi-n\varphi_0)}{\pi-n\varphi_0}\right] \quad n\neq\pm\pi/\varphi_0$$

$$F_3(\pm\pi/\varphi_0) = \pm\frac{\varphi_0^2}{8}[\mathrm{J}_1(2\pi)-\pi]$$

$$F_4(n) = \tfrac{1}{4}\left[\frac{3}{n}+\frac{4n}{(\pi/\varphi_0)^2-n^2}-\frac{n}{(2\pi/\varphi_0)^2-n^2}\right]\sin(n\varphi_0) \quad n\neq 0, n\neq\pm\pi/\varphi_0, n\neq\pm 2\pi/\varphi_0$$

$$F_4(0) = \tfrac{3}{4}\varphi_0$$

$$F_4(\pm\pi/\varphi_0) = \tfrac{1}{2}\varphi_0$$

$$F_4(\pm 2\pi/\varphi_0) = \tfrac{1}{8}\varphi_0$$

$$F_5(n) = \frac{\pi}{2\varphi_0}\left[\frac{1}{(2\pi/\varphi_0)^2-n^2}-\frac{1}{(\pi/\varphi_0)^2-n^2}\right]\sin(n\varphi_0) \quad n\neq\pm\pi/\varphi_0, n\neq\pm 2\pi/\varphi_0$$

$$F_5(\pm\pi/\varphi_0) = \mp\tfrac{1}{4}\varphi_0$$

$$F_5(\pm 2\pi/\varphi_0) = \mp\tfrac{1}{8}\varphi_0$$

$$F_6(n) = \frac{\pi}{16}\varphi_0^2\left[\frac{6\mathrm{J}_1(n\varphi_0)}{n\varphi_0}+\frac{4\mathrm{J}_1(\pi-n\varphi_0)}{\pi-n\varphi_0}+\frac{4\mathrm{J}_1(\pi+n\varphi_0)}{\pi+n\varphi_0}+\frac{\mathrm{J}_1(2\pi-n\varphi_0)}{2\pi-n\varphi_0}+\frac{\mathrm{J}_1(2\pi+n\varphi_0)}{2\pi+n\varphi_0}\right]$$

$$n\neq 0, n\neq\pm\pi/\varphi_0, n\neq\pm 2\pi/\varphi_0$$

$$F_6(0) = \tfrac{1}{16}\varphi_0^2[3\pi+8\mathrm{J}_1(\pi)+\mathrm{J}_1(2\pi)]$$

$$F_6(\pm\pi/\varphi_0) = \tfrac{1}{48}\varphi_0^2[6\pi+21\mathrm{J}_1(\pi)+6\mathrm{J}_1(2\pi)+\mathrm{J}_1(3\pi)]$$

$$F_6(\pm 2\pi/\varphi_0) = \tfrac{1}{192}\varphi_0^2[6\pi+48\mathrm{J}_1(\pi)+36\mathrm{J}_1(2\pi)+16\mathrm{J}_1(3\pi)+3\mathrm{J}_1(4\pi)]$$

$$F_7(n) = \frac{\pi}{16}\varphi_0^2\left[\frac{2\mathrm{J}_1(\pi+n\varphi_0)}{\pi+n\varphi_0}-\frac{2\mathrm{J}_1(\pi-n\varphi_0)}{\pi-n\varphi_0}-\frac{\mathrm{J}_1(2\pi-n\varphi_0)}{2\pi-n\varphi_0}+\frac{\mathrm{J}_1(2\pi+n\varphi_0)}{2\pi+n\varphi_0}\right] \quad n\neq\pm\pi/\varphi_0, n\neq\pm 2\pi/\varphi_0$$

$$F_7(\pm\pi/\varphi_0) = \pm\tfrac{1}{48}\varphi_0^2[(-3\pi-3\mathrm{J}_1(\pi)+3\mathrm{J}_1(2\pi)+\mathrm{J}_1(3\pi)]$$

$$F_7(\pm 2\pi/\varphi_0) = \pm\tfrac{1}{192}\varphi_0^2[-6\pi-24\mathrm{J}_1(\pi)+8\mathrm{J}_1(3\pi)+3\mathrm{J}_1(4\pi)].$$

The elements of the matrices $\mathrm{Re}\,\mathbf{R}_0$, $\mathrm{Re}\,\mathbf{R}_1^m$ and $\mathrm{Re}\,\mathbf{R}_2$ are obtained by replacing H_n and its derivatives by J_n, etc. in the expressions for $\mathbf{R}_0$, $\mathbf{R}_1^m$ and $\mathbf{R}_2$, respectively.